P1.1

REFLECTIVITY MEASUREMENT OF RAIN USING A 94 GHZ RADAR

Peter J. Speirs[1]*, David G. Macfarlane[1], Scott L. Cassidy[1]. Paul D. Cole[2], Melanie J. Froude[3] and Duncan A. Robertson[1]

1. University of St Andrews, St Andrews, Fife, UK.
2. Montserrat Volcano Observatory, Montserrat.
3. University of East Anglia, Norwich, UK.

1. INTRODUCTION

Whilst most rainfall radars operate in the Rayleigh regime by employing microwave signals (with centimetre wavelengths), in certain circumstances it can be advantageous to use millimeter-wave radars. Such radars can be, for the same antenna gain, far smaller than their lower frequency counterparts. With appropriately chosen architectures they can also be comparatively low power devices. These two factors make it possible for the systems to be man-portable and capable of being run from batteries, enabling operation far from mains power. Millimeter-wave radars can also potentially provide higher resolution data than their lower-frequency counterparts.

However, fundamental difficulties exist which make millimeter-wave radars less than ideally suited to measuring rain. Operating in the Mie scattering regime rather than the Rayleigh regime means that there is a far less pronounced increase in reflectivity as rainfall rate increases. Additionally, attenuation due to the rain is far higher, making the measurements more challenging, less precise and limiting the maximum range of measurement. Nonetheless, the advantages of compact low power systems offering high resolution mean that these drawbacks are worth tackling.

Additionally, it may sometimes be desirable to task an existing mm-wave radar to the measurement of rain. It is this situation that applies to the work discussed in this extended abstract. The Millimetre-Wave Group at St Andrews has two 94 GHz frequency-modulated continuous wave (FMCW) radars that are used to monitor the changing topography of the Soufriere Hills volcano on Montserrat (original system described in Robertson and Macfarlane, 2004). However, more recently, interest has developed in monitoring rainfall on the volcano, owing to the suggestion that for this type of volcano eruptions can sometimes be caused in part by heavy rainfall (Matthews et al, 2002). There is also interest in monitoring the rainfall in the Belham Valley with a view to predicting/monitoring lahars (mud flows).

In this work we describe the use of these terrain imaging radars for monitoring local rainfall, as well as showing preliminary results from measurements taken from another similar system at St Andrews.

2. THE RADARS

The two radars in Montserrat are part of the All-weather Volcano Topography Imaging Sensor series of instruments developed by the University of St Andrews: AVTIS-2 and AVTIS-3. The original instrument, AVTIS-1 was the predecessor to the current radars, and no longer exists. Both radars are 94 GHz FMCW radars. . AVTIS-2 is a portable radar designed to be set up for short periods of time at different locations, and is battery powered. AVTIS-3 is fixed in location, solar and battery powered and operates autonomously, with a wireless link to transmit data back to the Montserrat Volcano Observatory and is shown in figure 1. Due to its 24/7 availability and being deployed on the volcano, AVTIS-3 will principally be used for the rain measurements. Specifications for the two instruments are given in table 1 below.

Parameter	AVTIS-2	AVTIS-3
Transmit power	20 dBm	20 dBm
Antenna diameter	0.45 m	0.3 m
Antenna gain	51.4 dBi	46.2 dBi
3dB one-way beamwidth	0.5°	0.7°

Table 1 Pertinent specifications of the AVTIS radars

Figure 1 The AVTIS-3 radar system installed on Montserrat.

* *Corresponding Author Address:* Peter J. Speirs, School of Physics and Astronomy, University of St Andrews, North Haugh, St Andrews, Fife, KY16 9SS, Scotland.
+44 (0)1334 46 3079; e-mail: pjs27@st-andrews.ac.uk

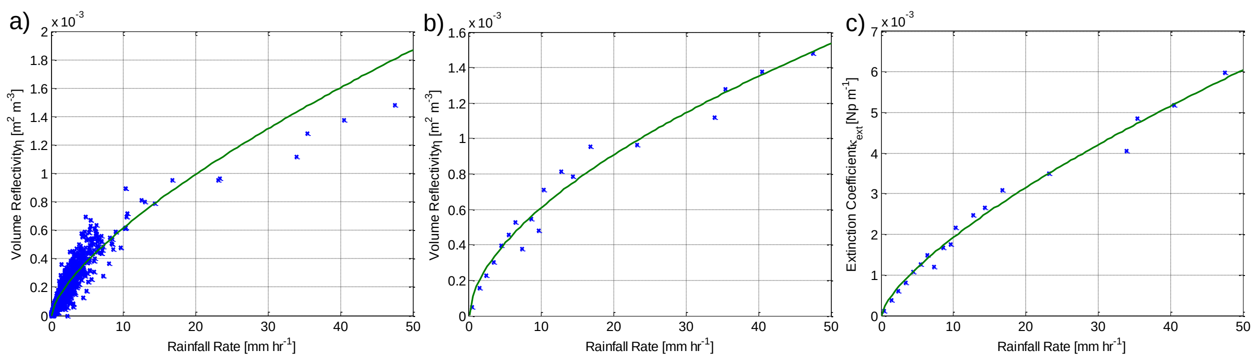

Figure 2 a) An aR^b curve fitted to the disdrometer-determined reflectivities plotted against rainfall rates. **b)** As in a), but with the DSDs averaged across 1 mm hr^{-1} intervals. **c)** An aR^b plot fitted to the calculated extinction coefficient from the averaged DSDs.

3. THE MEASUREMENT TECHNIQUE

The most appropriate measurement technique when using single frequency, single polarization radars is to relate the reflectivity directly to rainfall rate through a Z-R type relationship. Standard Z-R relationships make the assumption that the scattering from the raindrops lies in the Rayleigh region, which is not the case here. Indeed, the use of Z is largely a convenience for working between different frequencies in the Rayleigh regime, and is of less utility when working at higher frequencies. As a result, it will be necessary to develop new rainfall rate relationships, and these will be determined as η-R relationships (with η being the volume radar reflectivity).

Attenuation due to the rain is significant at millimetre wave frequencies and so must be taken into account. It has to be calculated progressively in range away from the radar as the attenuation in each range bin affects the measured reflectivity in all the more distant range bins. To account for this an η-κ_{ext} relation (where κ_{ext} is extinction) is also established. In principle, this would be applied to the first range bin and then used to determine a path attenuation to the second range bin. The second range bin measured reflectivity would then be corrected by this path attenuation, its own path attenuation calculated, and combined with the attenuation of the first range bin to calculate the reflectivity of the third range bin, and so on.

In practice however the radars used here will not be capable of accurately determining reflectivity very close to the radar due to being in the antenna near-field and the receiver response having a steep high-pass characteristic at short ranges. Consequently, it is necessary to assume that the rainfall rate is constant out to a range at which the reflectivity can be accurately measured. An η_{meas}-R curve can be calculated for this range bin on the assumption of constant rainfall rate over the path to this bin, and this then used as a starting point to work out from in the manner described.

This dependence of every subsequent rainfall rate measurement on the accuracy of the reflectivity of each preceding range bin inevitably means that errors build up, limiting this technique to comparatively short ranges.

4. DETERMINING THE RAINFALL RATE CURVES

The very high (and *a-priori* unquantifiable) levels of attenuation mean that it is not possible to construct the η-R curve directly from radar measurements and ground-based rainfall rate measurements. Instead, they have been constructed from disdrometer measurements of the rain. This has been done by fitting a normalized gamma distribution (Illingworth and Blackman, 2002) to the disdrometer data and then determining the theoretical reflectivity of this distribution, assuming Mie scattering from spherical raindrops. This allows the determination of a reflectivity associated with the DSD resulting in each rainfall rate. A curve of the form $\eta = aR^b$ is then fitted to the resultant calculated values, which is used in processing the rainfall data.

One slight complication is that there are often many more samples available over one particular range of rainfall rates (in St Andrews case, very large numbers of low rainfall rates measured compared with the rarer high rainfall rates). This acts as an indirect form of weighting in the fitting of the aR^b curve, as can be seen in the example St Andrews data in figure 2a).

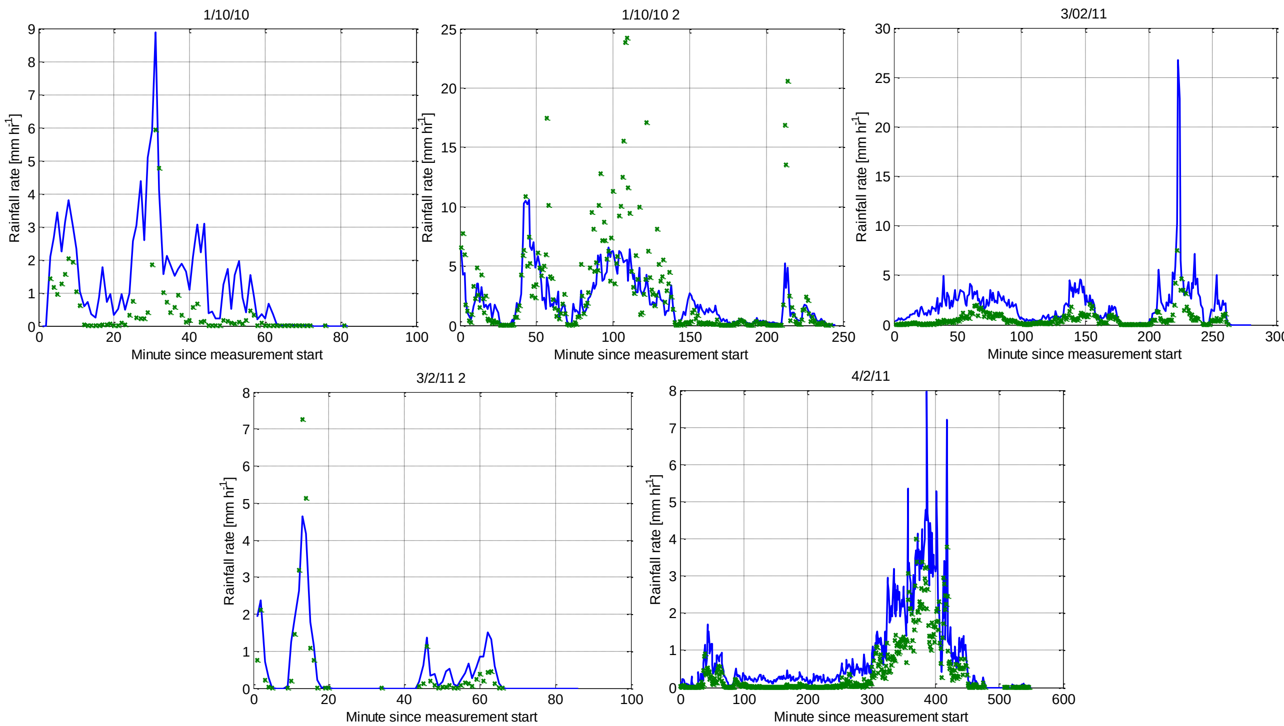

Figure 3 Samples of the radar derived rainfall rate (green crosses) plotted alongside the distrometer-measured rainfall rate (blue line). The radar derived measurements are from the range bin closest to 70m distant – i.e. the one closest to being directly above the disdrometer.

However, if instead of performing the normalized-gamma fitting for each measured DSD it is performed only on the average DSD for rainfall rates falling within each of a set of equal-sized rainfall rate value bins then this effect can be eliminated. In the particular case of the St Andrews data, the resulting $\eta = aR^b$ is shown in figure 2b), and the equivalent for the extinction coefficient in 2c).

The implementation is less than perfect as in some of the bins used, no rain was measured. There is additionally the problem that bins with DSDs produced from only a very small number of values may not be as representative of the longer term average behaviour of the rain as the bins in which many DSDs have been averaged.

5. THE ST ANDREWS EXPERIMENTAL SETUP

In order to test the feasibility of this technique, work has begun using a similar radar to that deployed in Montserrat. Measurements have been made across a large grass field in which a Thies laser disdrometer (www.thiesclima.com/disdrometer.html) was sited, at a distance of approximately 70 m from the radar, and below the radar beam. A weather station sited approximately 600 m from the radar and disdrometer was used to monitor temperature, and its tipping bucket gauge data was used to corroborate the rainfall rates measured by the disdrometer.

The radar used for these test measurements is a 94 GHz FMCW radar (known as “Bug-Eyes”), with the specifications listed in table 2. The system is still being refined, and over the data collection period reported here, three different data acquisition setups were used. However, all have been converted to measured-reflectivity, and averaged over the period of one minute, to match the measurement period of the laser disdrometer.

Parameter	“Bug-Eyes”
Transmit power	7.35 dBm
Antenna gain	40.45 dBi
3dB one-way beamwidth	1.485°

Table 2 Pertinent specifications for the “Bug-Eyes” radar.

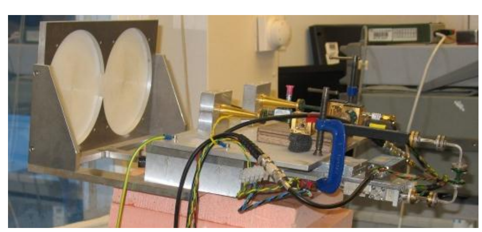

Figure 4 The “Bug-Eyes” radar.

6. PRELIMENARY ST ANDREWS RADAR RESULTS

Data collection is still ongoing, and so the rainfall rate curves produced should be considered as working curves rather than definitive ones. The current curves used are shown in figures 2b) and 2c).

With these curves, the data shown in figure 3 was processed. The radar calculated rainfall rates are shown against the disdrometer measured rainfall rates. It can be seen that, while the radar and disdrometer generally both report heavier and lighter rainfall rates in agreement, the actual numeric values have significant discrepancies. Some variation is to be expected to result from the variability in the DSD, but cannot account for the full extent of the variation seen.

Part of this can be attributed to noise, interference and possibly some non-linearity in the radar response. Slight problems, particularly close into the radar, can quickly be exacerbated by the method of calculating the cumulative path attenuation. Many of these problems are system-specific and are not a problem for the AVTIS systems, but they will need to be addressed before any more data from St Andrews is collected.

7. DATA MEASURED BY THE AVTIS SYSTEM

The AVTIS deployment is in some ways similar to the St Andrews deployment. A disdrometer has also been installed on Montserrat, and the data from it will be used in deriving the η-R curve. Unfortunately the disdrometer has no telemetry, and so is reliant on someone visiting the disdrometer and copying the data from a memory card. As a result, only a very small set of disdrometer data is available to date, not sufficient to derive any meaningful $\eta = aR^b$ curves. A great deal of rain data has already been collected using the AVTIS-3 radar, but so far it has not been possible to process this.

Some examples of the data obtained is shown in

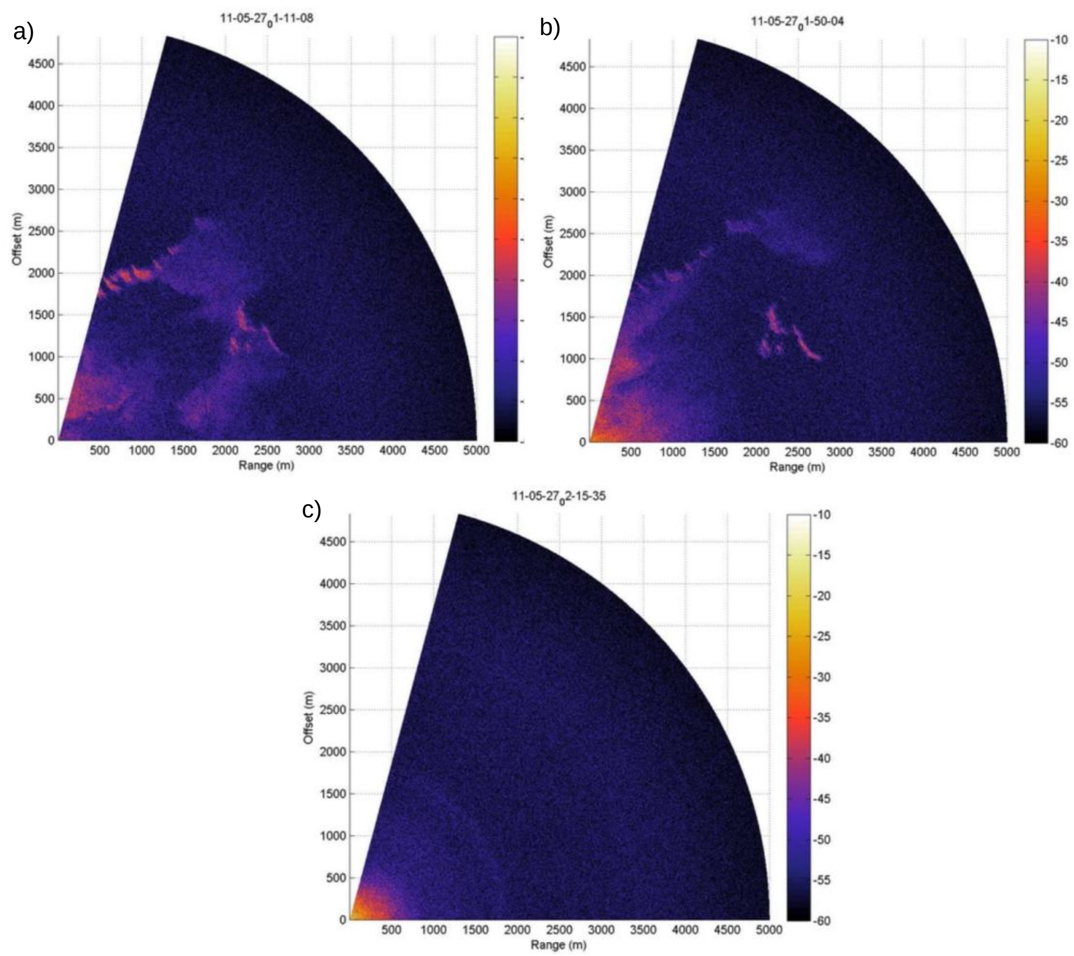

Figure 5 a) and **b)** show sample AVTIS-3 measurements made in rain. The sides of the Belham valley can clearly be seen, as can the locations of the rainshowers out to a range of several kilometers. **c)** Shows a sample measurement from AVTIS from a period where the rainfall was too heavy for AVTIS-3 to be able to measure.

figure 5. In a) and b), the rainfall can clearly be seen against the backdrop of the sides of the Belham valley, and some local “structure” in the rain can be seen. However in c), the rainfall rate resulted in too high an attenuation to allow the radar to measure it. Part of this may be due to wetting of the polystyrene radome.

8. OUTLOOK

More work is required to achieve the desired performance of the Bug-Eyes setup at St Andrews. Initially this is going to involve extensive recalibration of the radar system. Beyond that, it may become necessary to make use of the disdrometer data to correct the radar data. This is less than ideal, as to do the same on Montserrat for real-time observation would require telemetry to be added to the disdrometer. This would be possible, but difficult. Certainly, it should be possible to include the disdrometer data information in post-processing.

Full Montserrat data is expected to be available soon. This will be processed using a similar methodology to that used for the St Andrews data, and will be validated against the Montserrat disdrometer, the local tipping bucket gauges and possibly against data from the MeteoFrance weather radar on Guadeloupe.

9. REFERENCES

Illingworth, A. J., & Blackman, T. M. 2002: The Need to Represent Raindrop Size Spectra as Normalized Gamma Distributions for the Interpretation of Polarization Radar Observations. *J. Appl. Met ,* **41**, 286-297.

Matthews, A. J., Barclay, J., Carn, S., Thompson, G., Alexander, J., Herd, R. & Williams, C. 2002: Rainfall-induced volcanic activity on Montserrat. *Geophys. Res. Lett.*, **29**(13), 22-1 to 22-4.

Robertson, D. A. & Macfarlane, D. G. 2004: A 94GHz dual-mode active/passive imager for remote sensing. *Passive Millimetre-Wave Imaging Technology IX, Proc. SPIE*, **5619***, 621102.1-621102.10,* Orlando.